ANNALI DI GEOFISICA, VOL. 42, N. 2, April 1999

Measurements of vector magnetic anomalies on board the icebreaker Shirase and the magnetization of the ship

Yoshifumi Nogi and Katsutada Kaminuma
National Institute of Polar Research, Itabashi, Tokyo, Japan

Abstract
Vector measurements of the geomagnetic field have been made in the South Indian Ocean since 1988 when a Shipboard Three Component Magnetometer (STCM) was installed on board the icebreaker Shirase by the 30th Japanese Antarctic Research Expedition (JARE-30). Twelve constants related to the ship's induced and permanent magnetic field were determined by the data obtained from the JARE-30 to the JARE-35. The constants related to the ship's magnetic susceptibility distribution are almost stable throughout the cruise and mostly depend on the ship's shape. On the other hand, the constants related to the ship's permanent magnetization are variable. However, absolute values of total intensity geomagnetic field calculated from vector geomagnetic field is possible to use, if the constraints from total intensity geomagnetic field measured by the proton magnetometer and/or satellite derived magnetic anomalies are applied.

Key words *shipboard three component magnetometer – vector measurements of the geomagnetic field – ship's permanent magnetization – ship's induced magnetic field*

1. Introduction

Marine magnetic anomalies in the Southern Ocean are vital to understanding the geological processes involved in the breakup of Gondwana. However, marine magnetic data are still sparse and magnetic anomaly lineations remain undetermined, especially in the South Indian Ocean. Measurements of the vector geomagnetic field have been carried out by a Shipboard Three-Component Magnetometer (STCM; Isezaki, 1986) on board the Japanese icebreaker Shirase on her round cruise between Japan and Antarctica since the 30th Japanese Antarctic Research Expedition (JARE-30) in 1988-1989 for identifying magnetic anomaly lineations in the South Indian Ocean.

Vector measurements of the geomagnetic field with STCM provide more detailed information than measurements of total intensity with a proton magnetometer to reveal the magnetic structures of the oceanic crust. STCM was developed recently and used in many oceanic regions to measure geomagnetic field vectors successfully. Although sparse proton magnetometer observations do not identify the magnetic anomalies, the STCM vector geomagnetic anomalies allow us to infer the strike of two-dimensional magnetic structures, such as magnetic anomaly lineations and fracture zones, even with single observation line (Seama *et al.*, 1993). Moreover, STCM can easily be installed on any ships and operated even under severe weather conditions, because the sensors of this system can be fixed on the deck.

Relative change in total intensity geomagnetic field calculated from vector geomagnetic

Mailing address: Dr. Yoshifumi Nogi, National Institute of Polar Research, 1-9-10 Kaga, Itabashi, Tokyo 173-8515, Japan; e-mail: nogi@nipr.ac.jp

field obtained by STCM was in good agreement with that measured by the proton magnetometer (Isezaki, 1986; Nogi *et al.*, 1990; Korenaga 1995). However, absolute values of total intensity geomagnetic field calculated from vector geomagnetic field is not reliable at present. Therefore, absolute values of total intensity geomagnetic field calculated from vector geomagnetic field should be carefully used when merged into those measured by the proton magnetometer.

The status of vector geomagnetic field measurements by STCM on board Shirase since the JARE-30 (1988) are summarized in this paper. We also discuss that total intensity magnetic anomalies calculated from vector geomagnetic field merge into compilation of those obtained by the proton magnetometer, such as the Antarctic Digital Magnetic Anomaly Map (ADMAP).

2. Measurements on board the icebreaker Shirase

Observation lines of the measurements of the vector geomagnetic field on board Shirase from the JARE-30 (1988) to the JARE-38 (1996) are shown in fig. 1. The vector geomagnetic field is obtained along these observation lines using the method developed by Isezaki (1986). The strikes of the two-dimensional magnetic structures, such as magnetic anomaly lineation and fracture zone trends, are also determined according to the method shown by Seama *et al.* (1993). Nogi *et al.* (1992, 1996) have published some results of magnetic anomaly lineation and fracture trends in the Southern Indian Ocean deduced from the vector geomagnetic anomaly field as well as the sea surface and satellite gravity anomaly data.

Vector magnetic data ($\boldsymbol{H}_{ob}$) are obtained using three magnetic field components from orthogonal flux gate magnetometer sensors mounted on the ship's deck together with gyrocompass data to provide ship roll ($\boldsymbol{R}$), pitch ($\boldsymbol{P}$) and yaw ($\boldsymbol{Y}$). The ambient field vector $\boldsymbol{F}$, is given by

$$\boldsymbol{H}_{ob} = \boldsymbol{A} \cdot \boldsymbol{R} \cdot \boldsymbol{P} \cdot \boldsymbol{Y} \cdot \boldsymbol{F} + \boldsymbol{H}_p \qquad (2.1)$$

where $\boldsymbol{A}$ is a 3 × 3 matrix including the effect of the sensor's location and the ship's magnetic susceptibility distribution, and $\boldsymbol{H}_p$ is the magnetic field produced by the ship's permanent magnetic moment (Isezaki, 1986). Equation (2.1) can be transformed

$$\boldsymbol{B} \cdot \boldsymbol{H}_{ob} + \boldsymbol{H}_{pb} = \boldsymbol{R} \cdot \boldsymbol{P} \cdot \boldsymbol{Y} \cdot \boldsymbol{F} \qquad (2.2)$$

where $\boldsymbol{B}$ is $\boldsymbol{A}^{-1}$, and $\boldsymbol{H}_{pb}$ is $-\boldsymbol{A}^{-1} \cdot \boldsymbol{H}_p$ (Seama, 1992). $\boldsymbol{B}$ is also a non dimensional 3 × 3 matrix related to the effect of the sensor's location and the ship's magnetic susceptibility distribution. $\boldsymbol{H}_{pb}$ represents the time-independent bias component and the unit is in nT. Equation (2.2) is convenient form for calculating the vector geomagnetic field from observed data and usually used. Right side of eq. (2.2) is the conversion from the ship's fixed coordinate system to the Earth's fixed coordinate system. $\boldsymbol{B}$ and $\boldsymbol{H}_{pb}$ are expressed as follows.

$$\boldsymbol{B} = \begin{pmatrix} B_{11} & B_{12} & B_{13} \\ B_{21} & B_{22} & B_{23} \\ B_{31} & B_{32} & B_{33} \end{pmatrix} \qquad (2.3)$$

$$\boldsymbol{H}_{pb} = \begin{pmatrix} H_{pb_1} \\ H_{pb_2} \\ H_{pb_3} \end{pmatrix} \qquad (2.4)$$

$\boldsymbol{B}$ and $\boldsymbol{H}_{pb}$ (twelve constants) are estimated from least square inversion using a 360 degree rotation of the ship at a point where $\boldsymbol{F}$ is known. Since true $\boldsymbol{F}$ is almost unknown, International Geomagnetic Reference Field (IGRF) is usually used for estimating $\boldsymbol{B}$ and $\boldsymbol{H}_p$. If $\boldsymbol{B}$ and $\boldsymbol{H}_p$ are estimated, ambient field $\boldsymbol{F}$ is determined at any location using measured $\boldsymbol{H}_{ob}$, $\boldsymbol{R}$, $\boldsymbol{P}$ and $\boldsymbol{Y}$. The 360 degree rotation data of the ship are obtained on board Shirase at least more than four different locations during each cruise while the ship steer tight circles both clockwise and anticlockwise directions, so called «figure eight».

$\boldsymbol{B}$ and $\boldsymbol{H}_p$ estimated from the JARE-30 to the JARE-35 are summarized in table I. The loca-

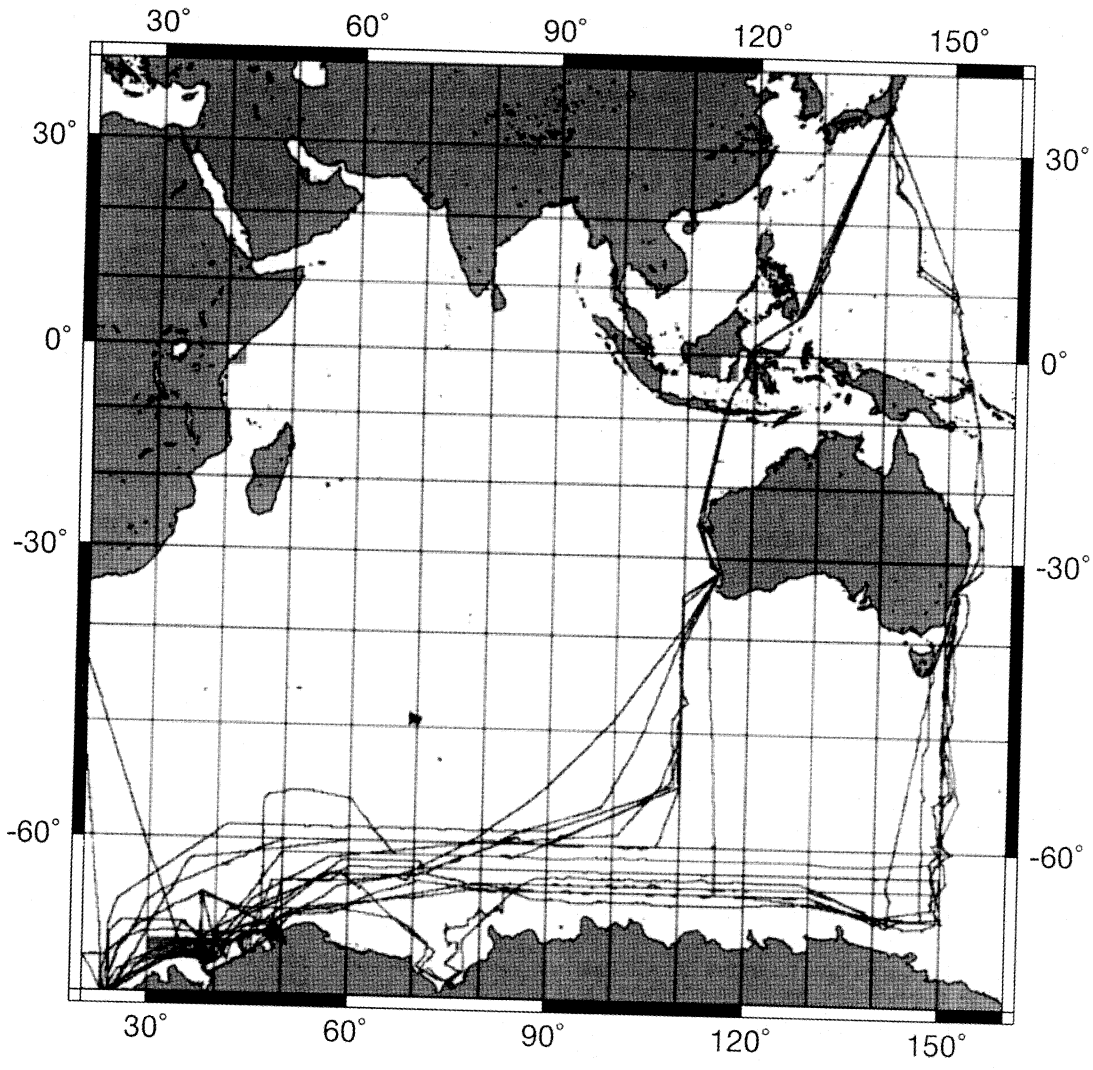

Fig. 1. Observation lines from the JARE-30 to the JARE-35.

tions where «figure eight» calibration was conducted are shown in fig. 2. The nine constants of $\boldsymbol{B}$ related to the ship's magnetic susceptibility distribution and the sensor's location are almost stable from the JARE-30 to the JARE-35. The variation of the nine constants of $\boldsymbol{B}$ depend on the change in the ship's magnetic susceptibility distribution, because the location of orthogonal flux gate magnetometer sensors have been fixed since those sensors mounted on the uppermost deck of Shirase in the JARE-30. The most effective constants, B_{11}, B_{22} and B_{33}, are nearly the same even the numbers of «figure eight» calibration varies from the JARE-30 to the JARE-35. The standard deviation of B_{11}, B_{22} and B_{33} ranges from 0.00112 to 0.00376. This corresponds to the filed change of 45 nT-150 nT in 40000 nT of the magnetic field. This result

Table I. The constants of $\boldsymbol{B}$ and $\boldsymbol{H}_{pb}$ estimated from the JARE-30 to the JARE-35. Num is the number of

	Num	b_{11}	b_{12}	b_{13}	b_{21}	b_{22}
JARE-30	5	1.12093	0.00861	0.03306	0.00027	1.36531
		(± 0.00030)	(± 0.00038)	(± 0.00017)	(± 0.00043)	(± 0.00054)
JARE-31	4	1.12340	0.00194	0.02335	0.00385	1.37385
		(± 0.00026)	(± 0.00032)	(± 0.00020)	(± 0.00033)	(± 0.00041)
JARE-32	8	1.12172	– 0.00301	0.04009	0.00826	1.37120
		(± 0.00082)	(± 0.00101)	(± 0.00063)	(± 0.00121)	(± 0.00150)
JARE-33	8	1.12187	0.00046	0.02875	0.00955	1.37150
		(± 0.00022)	(± 0.00028)	(± 0.00011)	(± 0.00033)	(± 0.00042)
JARE-34	6	1.12236	– 0.00256	0.02498	0.00999	1.37279
		(± 0.00027)	(± 0.00035)	(± 0.00012)	(± 0.00036)	(± 0.00046)
JARE-35	8	1.12393	0.00125	0.03390	0.00655	1.37658
		(± 0.00028)	(± 0.00037)	(± 0.00014)	(± 0.00035)	(± 0.00045)
Standard deviation		0.00112	0.00419	0.00624	0.00375	0.00376

indicate that the ship's magnetic susceptibility distribution is almost invariable throughout all the cruises.

The main role of Shirase is to carry all cargo and personnel to Japanese Antarctic Station, Syowa (69°S, 39°E), once a year. The total amount of the cargo and its items are changed every year. On her way back form Syowa Station to Sydney, Australia, the cargo store is almost empty throughout the cruise and the uppermost deck where the magnetic sensors are located far from the cargo stores in Shirase. The effect of the change in the amount and items of the cargo does not appear in the $\boldsymbol{B}$ values. These suggest that the effect of the ship's induced magnetic moment mostly depends on the ship's shape.

Estimated constants of $\boldsymbol{H}_{pb}$ are variable in contrast with the constants of $\boldsymbol{B}$ from the JARE-30 to the JARE-35. The standard deviation of $\boldsymbol{H}_{pb}$ is about 300 nT and this is almost three times larger than that of B_{11}, B_{22} and B_{33} in 40000 nT of the magnetic field. $\boldsymbol{H}_{pb}$ is $-\mathbf{A}^{-1} \cdot \boldsymbol{H}_p$ and the time-independent bias component. $\boldsymbol{B}$ ($\boldsymbol{A}^{-1}$) related to the ship's magnetic susceptibility distribution and the sensor's location is almost stable from the JARE-30 to the JARE-35 and indicates that the ship's magnetic susceptibility distribution is almost invariable throughout the cruises. Therefore $\boldsymbol{H}_{pb}$ almost represents the ship's permanent magnetic moment. This suggests that the ship's permanent magnetic moment varies every cruise.

3. Example of vector magnetic anomaly data

The observation line in the JARE-37 between Australia and Antarctica is shown in fig. 3. Figure 3 also shows the strike of two dimensional magnetic structure estimated from vector magnetic anomaly data using the method shown by Seama *et al.* (1993). Vector magnetic anomaly profile obtained along the observation line are shown in fig. 4. The strikes of two dimensional magnetic structures from vector magnetic anomalies are in good agreement with the strikes of

«figure eight» calibration. Estimated errors of $\boldsymbol{B}$ and $\boldsymbol{H}_{pb}$ are also indicated in parentheses.

b_{23}	b_{31}	b_{32}	b_{33}	H_{pb_1} (nT)	H_{pb_2} (nT)	H_{pb_3} (nT)
0.00407	0.08135	− 0.00425	0.89447	895.9	− 1295.3	− 1743.9
(± 0.00025)	(± 0.00046)	(± 0.00058)	(± 0.00026)	(± 8.9)	(± 12.8)	(± 13.6)
0.00920	0.08033	− 0.00520	0.89047	456.9	− 782.5	− 2004.2
(± 0.00025)	(± 0.00034)	(± 0.00041)	(± 0.00026)	(± 9.4)	(± 11.9)	(± 12.0)
0.01153	0.07204	0.00920	0.89096	954.5	− 407.6	− 1860.4
(± 0.00093)	(± 0.00056)	(± 0.00069)	(± 0.00043)	(± 31.7)	(± 46.7)	(± 21.6)
0.00645	0.07888	− 0.00663	0.89614	762.8	− 678.2	− 1150.2
(± 0.00017)	(± 0.00023)	(± 0.00029)	(± 0.00011)	(± 5.3)	(± 8.1)	(± 5.6)
0.01005	0.07979	− 0.00742	0.89234	299.7	− 811.6	− 1465.3
(± 0.00016)	(± 0.00031)	(± 0.00041)	(± 0.00015)	(± 6.1)	(± 8.0)	(± 7.1)
0.00791	0.07628	− 0.00792	0.89785	1283.7	− 712.7	− 1292.6
(± 0.00017)	(± 0.00016)	(± 0.00021)	(± 0.00008)	(± 6.7)	(± 8.3)	(± 3.9)
0.00856	0.00344	0.00647	0.00295	355.8	289.9	336.4

magnetic anomaly lineations previously identified in this area (*e.g.*, Cande *et al.*, 1989). This suggests that change in vector magnetic anomaly are correctly obtained.

Figure 4 shows the profile of vector magnetic anomalies and the ship's heading data. Vector magnetic field ($\boldsymbol{F}$) is calculated using the constants $\boldsymbol{B}$ and $\boldsymbol{H}_{pb}$ in the JARE-37. Total magnetic field is also computed from vector magnetic field ($\boldsymbol{F}$). Vector and total magnetic anomalies are obtained by subtracting the IGRF-95 (IAGA Division V, Working Group 8). The ship's course changes are indicated by dashed lines labeled with from A to E. X (northward) and Y (eastward) components of the magnetic field clearly change their DC components corresponding to the abrupt change of the ship's heading. A small change is also recognized in Z (downward) component when the ship's course change occur.

The DC level of Z component of the magnetic field gradually decreases in fig. 4. DC level of total intensity magnetic field calculated from vector magnetic anomalies increase. Variations of total intensity magnetic field from vector magnetic anomalies are similar to those of Z component, if variations of Z component are reversed. In the higher latitude, the Z component is dominant, and total intensity magnetic anomalies reflect almost all Z component magnetic anomalies. There is little contribution by X and Y components of magnetic anomalies in the higher latitude.

4. Discussion

Estimated constants of $\boldsymbol{B}$ related to the induced magnetic field of the ship's body are stable on board the icebreaker Shirase from the JARE-30 to the JARE-35. On the other hand, the constants of $\boldsymbol{H}_{pb}$ almost related to the permanent magnetic field of the ship's body is unstable. For determining the constants of $\boldsymbol{B}$ and $\boldsymbol{H}_{pb}$, IGRF is introduced as a known ambient magnetic field $\boldsymbol{F}$. IGRF does not reflect the true geomagnetic field especially in the high latitude

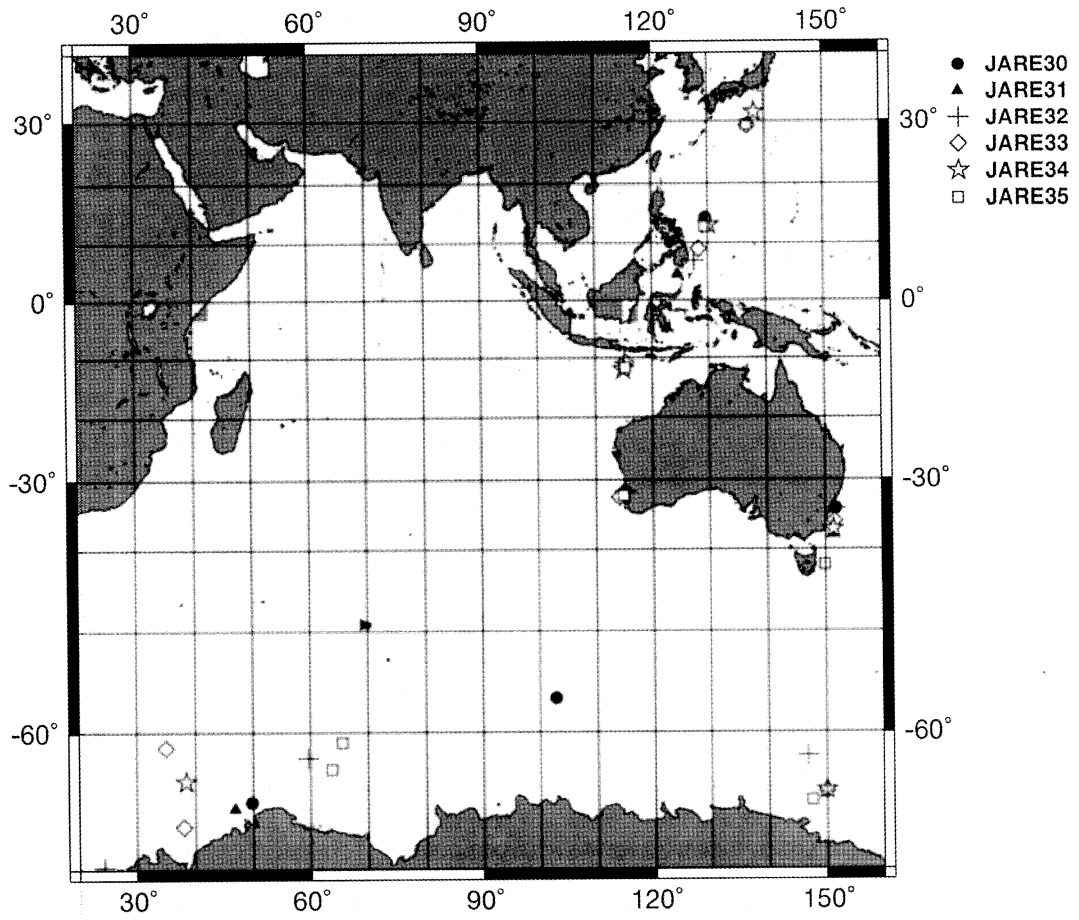

Fig. 2. Location where «figure eight» calibration was conducted from the JARE-30 to the JARE-35.

and ocean area. That is a possible cause for unstable constants of $\boldsymbol{H}_{pb}$. However, the constants of $\boldsymbol{B}$ are well determined throughout the cruise, and the locations, where «figure eight» calibrations were conducted, are widely distributed from the northern hemisphere to the southern hemisphere. The difference between IGRF and the true geomagnetic field will be canceled out by the widely distributed calibration points. Therefore the difference between IGRF and the true geomagnetic field is not the major cause for the unstable $\boldsymbol{H}_{pb}$.

The amount and the items of the cargo on board Shirase to supply the Syowa Station change every year. The change in the amount and items of the cargo on board Shirase is also a possible cause for variable constants of $\boldsymbol{H}_{pb}$ from the JARE-30 to the JARE-35. However, on her return back from Syowa Station to Sydney, Australia, the cargo store is almost empty throughout the cruise and the magnetic sensor's location on the deck is far from the cargo store on board Shirase. The effect of the change in the amount and items of the cargo does not appear in the constants of $\boldsymbol{B}$ either. The change in the amount and items of the cargo on board Shirase dose not seem to be a major cause for variable $\boldsymbol{H}_{pb}$ from the JARE-30 to the JARE-35.

The other possibility for the unstable constants of $\boldsymbol{H}_{pb}$ is the time-dependent component. The constants of $\boldsymbol{B}$ and $\boldsymbol{H}_{pb}$ are assumed to be time-independent constants. However, clear shifts of DC levels of X and Y components of the magnetic field are observed corresponding to the abrupt change of the ship's heading in fig. 4. A small change of the Z component also appeared corresponding to the ship's course change. Moreover, DC component of Z component magnetic field gradually decreases in fig. 4. The constants of $\boldsymbol{B}$ are stable throughout the cruise and indicate that the ship's magnetic susceptibility distribution is almost invariable throughout all the cruises. The constants of $\boldsymbol{H}_{pb}$ are determined as a time-independent DC levels of the magnetic field even if they show time-dependent components. This suggest that time-dependent change in DC level of the magnetic field, which is possibly the permanent magnetic

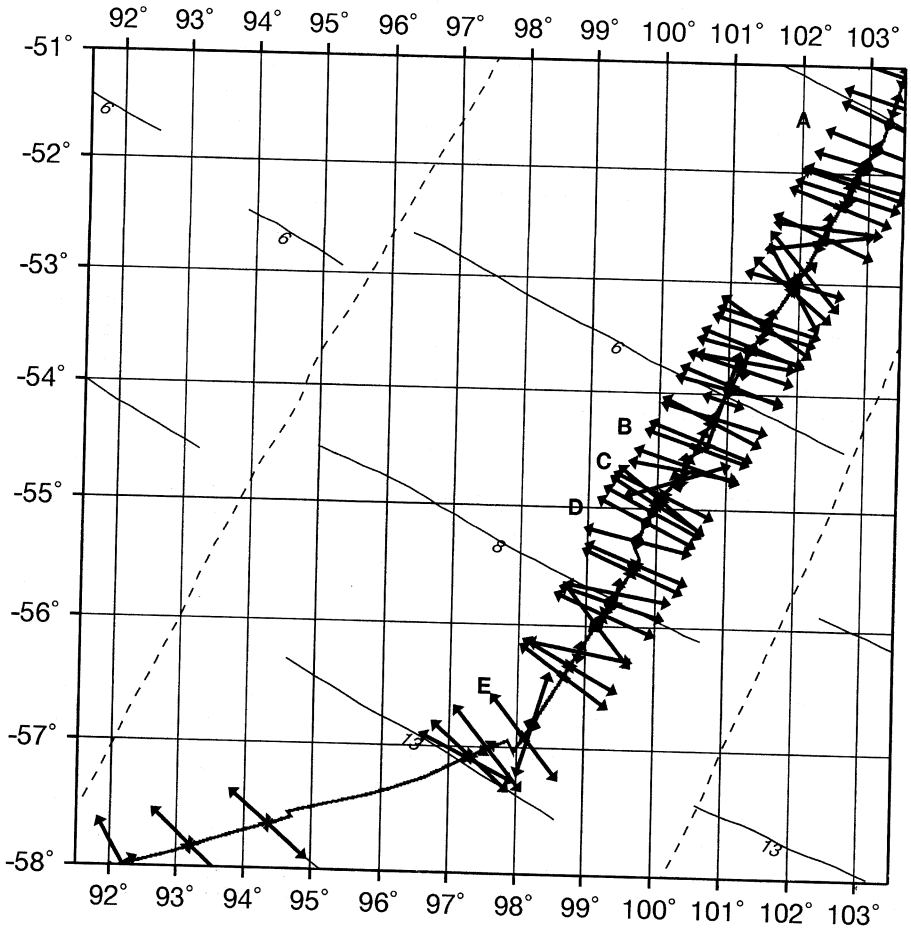

Fig. 3. Observation line in the JARE-37 between Australia and Antarctica (thick solid line). Cross arrows indicate the strikes of two dimensional magnetic structures calculated by using the method shown in Seama *et al.* (1993). Longer arrows show the strikes and shorter arrows show their standard deviation. Thin solid lines with number and dashed lines indicate previously identified magnetic anomaly lineations and fracture zones, respectively (Cande *et al.*, 1989). A-E indicate the major ship's course changes shown in fig. 4.

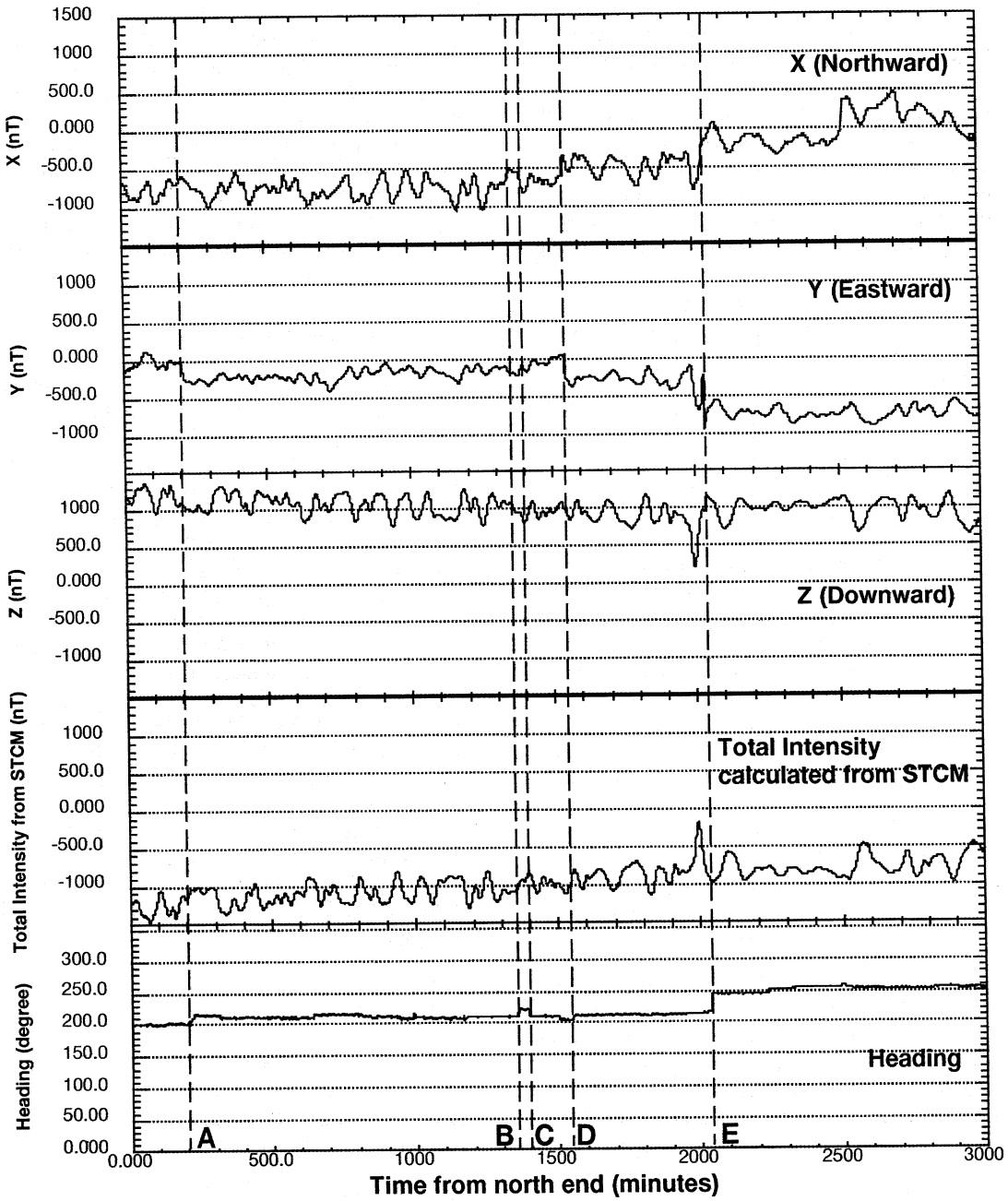

Fig. 4. Profiles of *X* (northward), *Y* (eastward) and *Z* (downward) components of the magnetic anomaly, total intensity geomagnetic field calculated from vector geomagnetic field after subtracting the IGRF-95 (IAGA Division V, Working Group 8, 1995) and the ship's heading data along the observation line in fig. 2.

field of the ship's body, is responsible for the variable $\boldsymbol{H}_{pb}$ from the JARE-30 to the JARE-35.

Viscous remanent magnetization of the ship's body is possibly the major factor responsible for unstable $\boldsymbol{H}_{pb}$ from the JARE-30 to the JARE-35. DC component of Z component magnetic field monotonously decrease in fig. 4. Apparently, this shows the permanent magnetic field of the ship's body gradually acquires an upward component of the magnetic field. The ship was sailing almost southward from Fremantle, Australia, to the Antarctic region and getting closer to the geomagnetic south pole. The direction of the ship's movement corresponds to the decrease in the Z component of the ambient magnetic field (downward positive). After the ship's major course change, the dashed line labeled with E in fig. 4, a clear increase or decrease in DC level of the Z component is not observed, possibly because the course of the ship turned to almost east-west direction and the Z component of the ambient magnetic field did not show large change. These variations could be explained by acquiring the viscous remanent magnetization of the ship's body.

No clear systematic decrease and increase of DC level are observed in X and Y components. X and Y components are more sensitive to the ship's course change than the Z component (one degree of the ship's heading change arise about 400 nT variation in X and Y components in the 25000 nT horizontal component of the magnetic field) and several DC shifts of X and Y components occurred in fig. 4 when the ship's course change happened. Therefore systematic increases or decreases in DC levels of X and Y components are not clear from DC level shifts of both components corresponding to the ship's course change. However, if X and Y components also acquire viscous remanent magnetization of the ship's body, these lead to an erroneous estimation of $\boldsymbol{H}_{pb}$. Erroneous estimation of $\boldsymbol{H}_{pb}$ also gives large DC shifts of X and Y component than that of Z component, because of the sensitivity of the rotation and assumption of time-independent $\boldsymbol{H}_{pb}$.

Total intensity of the geomagnetic field calculated from vector geomagnetic anomaly data can merge into the compilation of those obtained by the proton precession magnetometer. The effects of time-dependent component of $\boldsymbol{H}_{pb}$ and the heading change of the ship are a problem, but these effects can be almost easily removed by the following procedure. First, the observation lines are divided into some segments by the ship's major course change to avoid the DC level shifts in X, Y and Z components according to the ship's course change. Second, the linear trend of the variations of vector magnetic anomaly data along the each segmented observation line is removed. If viscous magnetization of the ship's body is a major factor of time-dependent variations in the ship's permanent magnetization, this effect could be observed as a linear trend. Relative change in total intensity geomagnetic field calculated from vector geomagnetic field by STCM was in good agreement with that measured by the proton magnetometer (Isezaki, 1986; Nogi *et al.*, 1990; Korenaga, 1995). The accuracy of relative change in vector magnetic field data almost depends on corrections of the induced magnetic field of the ship's body, and the constant of $\boldsymbol{B}$ are well determined throughout all the cruises. Moreover, the Z component is dominant in the higher latitude, and total intensity magnetic anomalies almost reflect Z component magnetic anomalies. The DC level shift in the Z component by the ship's heading change is smaller than those of X and Y components. Absolute value in the total intensity magnetic anomaly data calculated from vector magnetic anomalies will be obtained using the constraints from total intensity geomagnetic field measured by the proton magnetometer and/or satellite derived magnetic anomalies after above mentioned procedure.

5. Conclusions

Vector magnetic anomaly data obtained by STCM on board Shirase provide useful information in the South Indian Ocean where the magnetic data are sparse. Relative change of vector magnetic anomalies is reliable. Absolute values of total intensity geomagnetic field calculated from vector geomagnetic field should be used carefully when merged into those measured by the proton magnetometer. However, they can be used if the constraints from total intensi-

ty geomagnetic field measured by the proton magnetometer and/or satellite derived magnetic anomalies are applied. Further analysis for the ship's magnetization is required to determine the absolute values of total intensity geomagnetic field directly from the vector geomagnetic field obtained by STCM.

Acknowledgements

The authors thank the members from the JARE-30 to the JARE-38 and crews of the icebreaker Shirase for their kind help during operations. Y. N. thanks Prof. N. Isezaki and Dr. N. Seama , Chiba University, for numerous discussion. Comments by the reviewer Drs. C.E. Barton, F.J. Lowes and one anonymous reviewer improved the manuscript.

REFERENCES

CANDE, S.C., J.L. LABRECQUE, R.L. LARSON, W.C. PITMAN, III, X. GOLOVCHENKO and W.F. HAXBY (1989): *Magnetic Lineations of World's Ocean Basins (map)*, Amer. Ass. Petrol. Geol., Tulsa, OK.

IAGA DIVISION V, WORKING GROUP 8 (1995): International Geomagnetic Field, 1995 Revision, *J. Geomagn. Geoelectr.*, **47**, 1257-1261.

ISEZAKI, N. (1986): A new shipboard three component magnetometer, *Geophysics*, **51**, 1992-1998.

KORENAGA, J. (1995): Comprehensive analysis of marine magnetic vector anomalies, *J. Geophys. Res.*, **100**, 365-378.

NOGI, Y., N. SEAMA and N. ISEZAKI (1990): Preliminary report of three components of geomagnetic field measured on board the icebreaker Shirase during JARE-30, 1988-1989, *Proc. NIPR Symp. Antarct. Geosci.*, **4**, 191-200.

NOGI, Y., N. SEAMA and N. ISEZAKI (1992): The directions of magnetic anomaly lineations in Enderby Basin, off Antarctica, in *Recent Progress in Antarctic Earth Sciences*, edited by Y. YOSHIDA, K. KAMINUMA and K. SHIRAISHI (Terrapub, Tokyo), 649-654.

NOGI, Y., N. SEAMA, N. ISEZAKI and Y. FUKUDA (1996): Magnetic anomaly lineation and fracture zone formations deduced from vector data of the geomagnetic anomaly field in the West Enderby Basin adjacent to the Weddell Sea, in *Weddell Sea Tectonics and Gondwana Breakup*, edited by B.C. STOREY, E.C. KING and R.A. LIVERMORE, *Geol. Soc. Spec. Publ.*, **108**, 265-273.

SEAMA, N. (1992): Studies of vector geomagnetic anomalies in the oceans, *J. Jpn. Soc. Mar. Surv. Technol.*, **4**, 41-49 (in Japanese with English abstract).

SEAMA, N., Y. NOGI and N. ISEZAKI (1993): A new method for precise determination of the position and strike of magnetic boundaries using vector data of the geomagnetic anomaly field, *Geophys. J. Int.*, **113**, 155-164.